International Journal of Innovative Computing, Information and Control
Volume **18**, Number **2**, April **2022**

ICIC International ©2022 ISSN 1349-4198
pp. 537–550

MODEL PREDICTIVE CONTROL METHOD FOR WARSHIP DC MICRO-GRID BASED ON FINITE CONTROL SET

Zeliang Hao[1], Youqin Chen[1], Tinglong Pan[1,*], Weilin Yang[1] and Xichao Zhou[2]

[1]School of Internet of Things Engineering
Jiangnan University
No. 1800, Lihu Avenue, Wuxi 214122, P. R. China
{ 6191905019; 6191915001 }@stu.jiangnan.edu.cn; wlyang@jiangnan.edu.cn
*Corresponding author: tlpan@jiangnan.edu.cn

[2]Science and Technology Research and Development Center
State Grid Integrated Energy Service Group Co., Ltd.
No. 1, Baiguang Road, Xicheng District, Beijing 100053, P. R. China
zhouxichao@sgecs.sgcc.com.cn

Received August 2021; revised November 2021

Abstract. *There are a lot of electronic pulse loads in warship DC micro-grid, which makes the DC bus voltage fluctuate greatly and reduces the power supply quality of the equipment. In order to solve this problem, the hybrid energy storage system is used into the warship DC micro-grid in this paper. Based on the established warship DC micro-grid mathematical model, a model predictive control method based on finite control set (FCS-MPC) is designed for the power converters of micro-grid, and the power tracking control of each energy storage unit is realized. In the proposed FCS-MPC, the least square method is used to optimize the cost function. Simulation results in Matlab/Simulink show that the proposed control method has good effectiveness and advantages in stabilizing DC bus voltage, reducing regulation time and accelerating load response speed.*
Keywords: Hybrid energy storage system, Warship DC micro-grid, Model predictive control, Finite control set, The least squares

1. **Introduction.** There are usually various loads in war-ship DC distribution network. In addition to the propeller for navigation and the service load for normal operation of equipment, there are also high dynamic pulse loads that require a lot of power in a short time, such as electromagnetic ejection system, electronic laser weapons and radar [1,2]. The sudden acceleration and deceleration of warship and the use of electromagnetic weapons bring about a load change rate that far exceeds the climbing power of the generator. It will be difficult for the generator to quickly output sufficient power, which will inevitably lead to the imbalance between power generation and power consumption in the DC distribution network, resulting in DC bus voltage fluctuation, voltage distortion and frequency oscillation of generator output. More seriously, it will threaten the stable operation of the whole system. In order to solve this problem, energy storage devices are often used into DC distribution network to compensate power difference, stabilize DC bus voltage and improve power quality [3,4]. The generator and energy storage devices in the warship DC micro-grid are connected to the DC bus through their respective converters. Therefore, designing an efficient control strategy for these power converters so that the

DOI: 10.24507/ijicic.18.02.537

generator and energy storage system can output the reference power accurately is essential for improving the stability of the warship's DC bus voltage [5,6].

At present, many researchers have done a lot of research work on the control problems of these power converters. In [7] a dynamic evolution controller is designed for DC/DC converters, which enables super capacitors to quickly output electrical energy to compensate for the lack of dynamic response of fuel cells. In [8] a model predictive controller is designed, which ensures that the DC-DC converter has lower cross regulation in continuous conduction mode and improves the fast response of the reference voltage. For voltage source rectifier (VSR) converter, currently widely used technologies include feedback linearization [9], sliding mode variable structure control [10], direct power control [12], and passive control [13], etc.

Rodriguez et al. first proposed the control idea of FCS-MPC in the converter, applied it to the current predictive control of three-phase voltage source inverter, and achieved good results [14]. In [15], the basic principle of FCS-MPC is systematically described, and FCS-MPC is compared with traditional PI control to reflect its excellent characteristics compared with the traditional control. At the same time, corresponding objective performance functions are proposed for different converter topologies, showing the flexibility and universality of FCS-MPC application.

Predictive control is divided into continuous control set model predictive control (CCS-MPC) and finite control set model predictive control (FCS-MPC) according to different optimization methods and action modes. CCS-MPC is developed from the classical MPC. By analyzing the system state value and system state model at the current time, and analyzing and calculating all continuously rotating space voltage vectors on the complex plane, the required target output voltage is obtained. FCS-MPC selects the optimal predictive value after traversing and selecting limited control variables. CCS-MPC is different from FCS-MPC, and its control variables have more computation. Although the control accuracy is more accurate, there is a problem of large prediction error when the system is disturbed. FCS-MPC, which considers the objective optimization and switch state decision-making process as a whole, has the advantages of wide application range and simple application, so it has become a research hotspot of predictive control method. At present, there is little research on FCS-MPC in ship DC microgrid predictive control, so whether it can be introduced into ship system?

In view of this, this paper uses the hybrid energy storage system into the warship micro-grid system to make up for the insufficient output of the generator. Then, the finite control set model predictive control (MPC) is applied to the control of power converters in warship DC micro-grid system. The current is predicted, the cost function is designed combined with the load demand, and the least square method is used to solve it, so as to obtain the optimal switch combination state, which finally acts on the power converter and responds to the load demand quickly.

The rest of the article is divided into the following sections. In Section 2, the model of ship system is established. Section 3 illustrates the problem of ship energy allocation while Section 4 describes the controller design in detail. In Section 5, simulation results and analysis are given. Section 6 gives some conclusions.

2. **Warship DC Micro-Grid with Hybrid Energy Storage System.**

In order to reduce the negative impact of pulse load mutation on the voltage of warship DC bus, the hybrid energy storage system composed of super capacitor and battery is used into the micro-grid system, in which the generator is connected to the DC bus through VSR, and the energy storage unit is connected to the bus through DC-DC converter. The basic structure of warship DC micro-grid is shown in Figure 1.

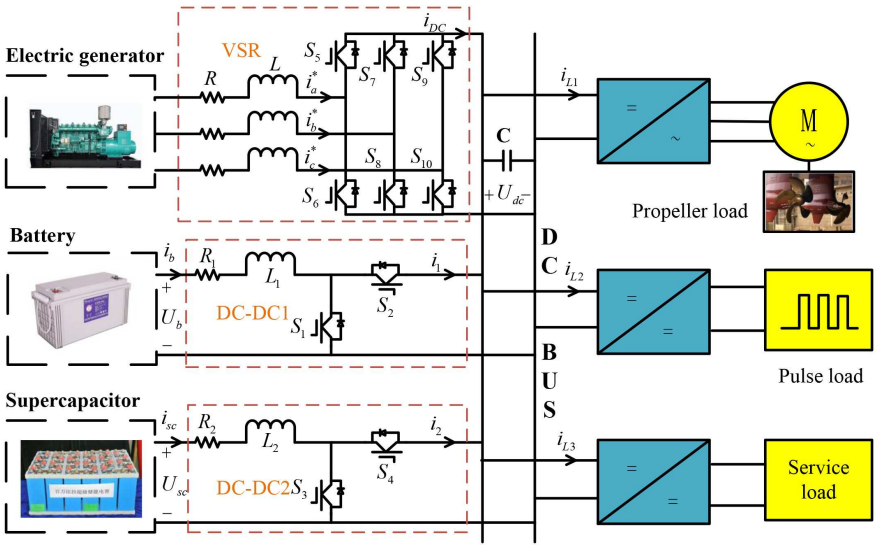

FIGURE 1. The basic topology of the warship's DC micro-grid

As shown in Figure 1, i_a^*, i_b^*, i_c^* are the three-phase current output by the generator. U_{dc} and i_{DC} are the DC bus voltage and current respectively. U_b, U_{sc}, i_b and i_{sc} are the voltage and current of the battery and super capacitor respectively. i_1 and i_2 are the current output of the battery and super capacitor through the DC-DC converter. i_{L1}, i_{L2} and i_{L3} are load currents of three different types of loads. C is the capacitance between DC bus. R and L are the equivalent resistance and inductance of the generator. R_1 and L_1 are the equivalent resistance and inductance of the battery. R_2 and L_2 are the equivalent resistance and inductance of the super capacitor.

2.1. **Mathematical model of VSR.** VSR is a device that converts AC power output by a synchronous generator into DC power. In order to simplify the design of the controller, it is assumed that the switch tube in the converter is ideal and has no power loss.

The model is transformed into the two-phase rotating d-q coordinate system through coordinate transformation, and the following results can be obtained:

$$\begin{cases} Ldi_d/dt = E_d - Ri_d + \omega Li_q - m_d U_{dc} \\ Ldi_q/dt = E_q - Ri_q + \omega Li_d - m_q U_{dc} \end{cases} \tag{1}$$

where E_d, E_q, i_d, i_q are respectively the voltage and current of the generator in the coordinate system d-q, and m_d, m_q are the switching functions in the d-q coordinate system. ω is the synchronous frequency, and R, L are the equivalent resistance and inductance in the circuit.

2.2. **The working mathematical model of the battery.** As the energy storage unit in the DC micro-grid, the battery is a device that can be discharged cyclically. Because the battery voltage is different from the DC bus voltage level, a bidirectional DC-DC converter is required to complete the task of voltage conversion and energy transmission. There are two working modes as follows.

When the battery is discharged, energy is transferred to the DC bus through the converter. Since the battery terminal voltage is lower than the DC bus voltage, the converter works in boost mode. At this time, S_2 is turned off and S_1 is chopped.

$$\begin{cases} i_b^* > 0, \\ i_1 = (1 - m_1)i_b, \\ di_b/dt = -(R_1/L_1)i_b + (1/L_1)U_b - ((1 - m_1)/L_1)U_{dc} \end{cases} \tag{2}$$

where i_b^* is the current reference value of the battery, i_b is the working current of the battery, U_b is the working voltage of the battery, m_1 is the switching function of the switch tube S_1, the value is 0 or 1, and i_1 is the output current of bidirectional DC-DC1. When the battery is charging, the converter should work in step-down mode, at this time S_1 is closed and S_2 is chopped.

$$\begin{cases} i_b^* < 0, \\ i_1 = m_2 i_b, \\ di_b/dt = -(R_1/L_1)i_b + (1/L_1)U_b - (m_2/L_1)U_{dc} \end{cases} \tag{3}$$

where m_2 is the switching function of the switch tube S_2, and the value is 0 or 1. In summary, the mathematical model of battery operation can be obtained:

$$\begin{cases} i_1 = m_{12} i_b, \\ m_{12} = \begin{cases} 1 - m_1 i_b^* > 0, \\ m_2 i_b^* < 0 \end{cases} \\ di_b/dt = -(R_1/L_1)i_b + (1/L_1)U_b - (m_{12}/L_1)U_{dc} \end{cases} \tag{4}$$

In the formula, m_{12} is the switching function of the battery, and the value is 0 or 1.

2.3. **The working mathematical model of super capacitor.** Both super capacitor and storage battery are voltage source devices. Compared with battery, super capacitor has high power density and fast charging and discharging speed, so it is very suitable for high power pulse load. The energy transmission between it and DC micro-grid is also completed by DC-DC converter, so its working mathematical model is similar to that of battery, as shown below:

$$\begin{cases} i_2 = m_{34} i_{sc}, \\ m_{34} = \begin{cases} 1 - m_3 i_{sc}^* > 0, \\ m_4 i_{sc}^* < 0 \end{cases} \\ di_{sc}/dt = -(R_2/L_2)i_{sc} + (1/L_2)U_{sc} - m_{34}/L_2 U_{dc} \end{cases} \tag{5}$$

where U_{sc} is the terminal voltage of the super capacitor, i_{sc} is the working current of the super capacitor, i_{sc}^* is the reference current of the super capacitor, m_3 and m_4 are the switching functions of S_3 and S_4 respectively, and their values are 0 or 1, and i_2 is the output current of bidirectional DC-DC2. In the formula, m_{34} is the switching function of the super capacitor, and the value is 0 or 1.

2.4. **The overall mathematical model of power converters.** According to Kirchhoff's current law, the voltage U_{dc} across the bus capacitor and the load current i_L have the following relationship:

$$dU_{dc}/dt = (i_{DC} + i_1 + i_2 - i_L)/C \tag{6}$$

where i_L is the load current. According to the law of power conservation, there is an equal relation warship between the active power of the AC measurement and the DC side of the VSR:

$$U_{dc} i_{DC} = \frac{3}{2}(E_d i_d + E_q i_q) \tag{7}$$

When the generator terminal voltage is stable, $E_q = 0$, substituting (7) into (6), we can get

$$dU_{dc}/dt = ((3E_d i_d)/(2U_{dc}) + m_{12} i_b + m_{34} i_{sc} - i_L)/C \tag{8}$$

The overall mathematical model of the power converter can be obtained from the above equation:

$$\begin{cases} di_d/dt = \delta_1 E_d - \delta_2 i_d + \omega i_q - \delta_1 m_d U_{dc} \\ di_q/dt = \delta_1 E_q - \delta_2 i_q - \omega i_d - \delta_1 m_q U_{dc} \\ di_b/dt = \delta_3 U_b - \delta_4 i_b - \delta_3 m_{12} U_{dc} \\ di_{sc}/dt = \delta_5 U_{sc} - \delta_6 i_{sc} - \delta_5 m_{34} U_{dc} \\ dU_{dc}/dt = \delta_7((3E_d i_d)/(2U_{dc}) + m_{12} i_b + m_{34} i_{sc} - i_L) \end{cases} \tag{9}$$

where $\delta_1 = 1/L$, $\delta_2 = R/L$, $\delta_3 = 1/L_1$, $\delta_4 = R_1/L_1$, $\delta_5 = 1/L_2$, $\delta_6 = R_2/L_2$, $\delta_7 = 1/C$. These parameters are determined by the resistance and capacitance of each converter in the DC micro-grid.

2.5. **Mathematical model of warship propeller load.** The loads in the warship system are roughly divided into the following three categories according to their purposes: thruster loads P_t, pulsed power loads P_h, and service loads P_s. Propeller drives propellers to rotate in the water and interact with the water to generate the power of the warship's navigation, which accounts for the largest proportion. In still water navigation, the relation warship between propeller power and speed is shown as Equation (10).

$$P_t = 2\pi sig(n) k_t \rho n^3 D^5 \tag{10}$$

where $sig(*)$ is the sign function, k_t is the coefficient of resistance torque, ρ is the density of seawater, n is the speed of propeller, and D is the diameter of propeller.

Pulse-type loads are generated by the use of electromagnetic weapons, and have the characteristics of short duration and rapid rate change. Service-type loads are the basis for maintaining the normal operation of warships. They usually supply electricity for daily use and electronic products without major fluctuations.

3. **Design of the Power Distribution Strategy in the Warship DC Micro-Grid.** In the sea navigation, in case of emergency, the warship needs to stop or accelerate or decelerate. At this time, the propeller needs to act quickly, which will produce a large fluctuation of propulsion load. In addition, the use of high-energy equipment such as electromagnetic weapons will bring pulse load. This rapidly changing load requires rapid response, but the climbing power of the generator is limited, and the regulation capacity is not enough to maintain the balance between power generation and power consumption, resulting in the fluctuation of bus voltage.

In order to solve this contradiction, the hybrid storage unit composed of battery and super capacitor is introduced into the warship DC micro network to make up for the insufficient output of generator. The battery has high energy density and low power density, which bears the low frequency components in the differential power. The super capacitor has high power density, high charging and discharging speed, and it bears the high frequency component in the differential power. The specific energy management strategies in the warship DC micro network system are as follows.

Firstly, the change rate $\Delta P_g^L(t)$ of the load demand $P_L^*(t)$ relative to the output of the generator $P_g(t - T_s)$ at the previous sampling time is calculated:

$$\Delta P_g^L(t) = (P_L^*(t) - P_g(t - T_s))/T_s \tag{11}$$

According to the value of load change rate $\Delta P_g^L(t)$, the following two cases are delimited.

Case1: $\Delta P_g^L(t) \leq P_{c,g}$, when the load demand change rate does not exceed the generator's climbing power, the load power is borne by the generator at this time, and the

power commands of each unit as follows:

$$P_g^*(t) = P_L^*(t),\ P_b^*(t) = 0,\ P_{sc}^*(t) = 0 \tag{12}$$

Case2: $\Delta P_g^L(t) > P_{c,g}$, when the change rate of load demand exceeds the climbing power of the generator, the hybrid energy storage system assumes the differential power $P_e^*(t)$, where the power instruction of the battery is the low-frequency component $P_e^{lf}(t)$ of the differential power passing through the first-order low-pass filter. The high frequency component $P_e^{hf}(t)$ is borne by the super capacitor.

$$\begin{cases} P_g^*(t) = P_g(t - T_s) + sig\left(\Lambda P_g^L(t)\right) P_{c,g} T_s \\ P_e^*(t) = P_L^*(t) - P_g^*(t) = P_e^{lf}(t) + P_e^{hf}(t) \end{cases} \tag{13}$$

where $P_e^{lf}(t) = P_b^*(t) = \vartheta P_e^*(t) + (1 - \vartheta) P_e^{lf}(t - T_s)$, $P_e^{hf}(t) = P_{sc}^*(t) = P_e^*(t) - P_e^{lf}(t)$, $\vartheta = T_s/(\tau + T_s)$, τ is the time constant of the first order low pass filter, and T_s is the sampling time.

The mathematical model of the warship's DC micro-grid takes current and voltage as the state quantity, so it is necessary to convert the reference power instruction of the battery and the super capacitor into reference current instruction:

$$i_{sc}^* = P_{sc}^*/U_{sc}^*,\ i_b^* = P_b^*/U_b^* \tag{14}$$

4. Controller Design.

4.1. **FCS-MPC strategy.** The principle of warship DC micro-grid finite control set current collection model predictive controller proposed in this paper is shown in Figure 2. The load power demand P_L^* is decomposed into high-frequency power and low-frequency power after passing through the power distribution unit. The high-frequency part corresponds to the super capacitor power demand P_{sc}^* and the low-frequency part corresponds to the battery power demand P_b^*. They are divided by their respective voltages U_{sc}, U_b to obtain their reference current i_{sc}^*, i_b^*. The reference currents of the generator in two-phase rotating d-q coordinate system are i_d^*, i_q^*. The current sampling values at the current time are i_{sc}^k, i_b^k, i_d^k, i_q^k respectively. After the prediction model, the current values at the next time are predicted to be i_{sc}^{k+1}, i_b^{k+1}, i_d^{k+1}, i_q^{k+1} respectively. According to the reference current value and the sampling predicted current value, the cost function J can be designed, and then transformed into the least square problem for solution, so as to obtain the optimal switch S_j combination, so as to control the operation of the converter.

The three-phase two-level inverter for the generator has 8 voltage vectors, which are respectively composed of 6 non-zero vectors $U_1[0,0,1]$, $U_2[0,1,0]$, $U_3[0,1,1]$, $U_4[1,0,0]$, $U_5[1,0,1]$, $U_6[1,1,0]$ and two zero vectors $U_0[0,0,0]$, $U_7[1,1,1]$. Eight current prediction values can be obtained by eight switch combinations, of which the current prediction values obtained by two zero vectors are the same, and finally seven current prediction values are obtained. For super capacitor and battery, there are three voltage vectors, $U_8[0,0]$, $U_9[0,1]$, $U_{10}[1,0]$. Through the above different current prediction values and relevant constraints, the output switching state and the total number of switching states at the next time can be obtained. Finally, 63 switching states can be obtained. According to Euler's equation, we can get the differential form of the current:

$$\begin{cases} di_d(t)/dt \approx (i_d(t_{i+1}) - i_d(t_i))/\Delta t \\ di_q(t)/dt \approx (i_q(t_{i+1}) - i_q(t_i))/\Delta t \\ di_b(t)/dt \approx (i_b(t_{i+1}) - i_b(t_i))/\Delta t \\ di_{sc}(t)/dt \approx (i_{sc}(t_{i+1}) - i_{sc}(t_i))/\Delta t \end{cases} \tag{15}$$

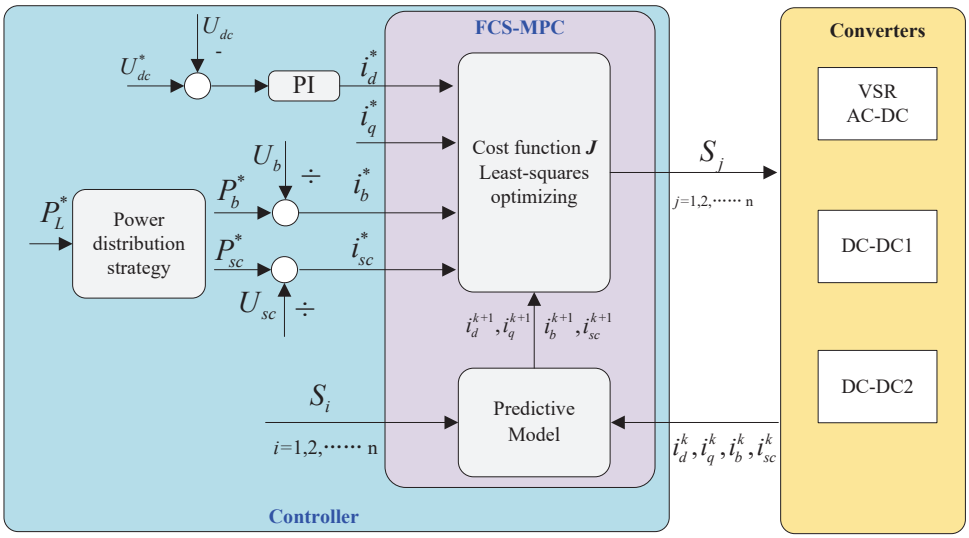

FIGURE 2. Schematic diagram of FCS-MPC controller

Therefore, the current value of the $k+1$ period can be obtained from the k period:

$$\begin{bmatrix} i_d^p(k+1) \\ i_q^p(k+1) \\ i_b^p(k+1) \\ i_{sc}^p(k+1) \end{bmatrix} = A(k) \begin{bmatrix} i_d^p(k) \\ i_q^p(k) \\ i_b^p(k) \\ i_{sc}^p(k) \end{bmatrix} + B(k) \begin{bmatrix} u_d(k) \\ u_q(k) \\ u_b(k) \\ u_{sc}(k) \end{bmatrix} + F(k) \tag{16}$$

where

$$A(k) = \begin{bmatrix} 1-T\delta_2 & T\omega(k) & 0 & 0 \\ -T\omega(k) & 1-T\delta_2 & 0 & 0 \\ 0 & 0 & 1-T\delta_4 & 0 \\ 0 & 0 & 0 & 1-T\delta_6 \end{bmatrix} \tag{17}$$

$$B(k) = \begin{bmatrix} T\delta_1 & 0 & 0 & 0 \\ 0 & T\delta_1 & 0 & 0 \\ 0 & 0 & T\delta_3 & 0 \\ 0 & 0 & 0 & T\delta_5 \end{bmatrix} \tag{18}$$

$$F(k) = \begin{bmatrix} -T\delta_1 \mathrm{m}_d U_{dc}(k) \\ -T\delta_1 \mathrm{m}_q U_{dc}(k) \\ -T\delta_3 \mathrm{m}_{12} U_{dc}(k) \\ -T\delta_5 \mathrm{m}_{34} U_{dc}(k) \end{bmatrix} \tag{19}$$

Equation (16) can be expressed as

$$x(k+1) = A(k)x(k) + BU(k) + F(k) \tag{20}$$

4.2. **FCS-MPC strategy based on least square method.** Assuming that the generator output power remains unchanged in the prediction range, the vector form of current prediction values in rolling time domain can be obtained [17]:

$$x(l+1) = A^{l-k+1}(k)x(k) + \left[A^{l-k}B\Lambda\right] U'(k) + \left[A^{l-k}F(k) + \cdots + A^0 F\right] \tag{21}$$

where $l = k, \ldots, k+N-1$ is the number of prediction steps, which can be obtained by writing it as the equation of state:

$$Y(k) = X(k) = \Gamma x(k) + \Upsilon U'(k) + \Pi \tag{22}$$

where

$$\Upsilon = \begin{bmatrix} B\Lambda & 0 & \dots & 0 \\ AB\Lambda & B\Lambda & \dots & 0 \\ \vdots & \vdots & \vdots & \vdots \\ A^{N-1}B\Lambda & A^{N-2}B\Lambda & \dots & B\Lambda \end{bmatrix} \tag{23}$$

$$\Gamma = \left[A, A^2, \dots, A^N\right]^{\mathrm{T}} \tag{24}$$

$$\Pi = \left[F, AF + F, \dots, \sum_{j=0}^{N-1} A^j F\right]^{\mathrm{T}} \tag{25}$$

$$\begin{aligned} U'(k) = [&\underbrace{U_1, U_2, U_3, U_4, U_5, U_6, U_7}_{v(k)^{\mathrm{T}}}, \underbrace{U_8, U_9, U_{10}, U_{11}, U_{12}, U_{13}, U_{14}}_{v(k+1)^{\mathrm{T}}}, \dots, \\ &\underbrace{U_{7N-6}, U_{7N-5}, U_{7N-4}, U_{7N-3}, U_{7N-2}, U_{7N-1}, U_{7N}}_{v(k+N-1)^{\mathrm{T}}}]^{\mathrm{T}} \end{aligned} \tag{26}$$

$$\Lambda = \begin{pmatrix} \cos(\phi_e(l)) & \sin(\phi_e(l)) & 0 & 0 \\ -\sin(\phi_e(l)) & \cos(\phi_e(l)) & 0 & 0 \\ 0 & 0 & 1 & 0 \\ 0 & 0 & 0 & 1 \end{pmatrix} \cdot \frac{2}{3} \cdot \begin{pmatrix} 1 & -\frac{1}{2} & -\frac{1}{2} & 0 & 0 & 0 & 0 \\ 0 & \frac{\sqrt{3}}{2} & -\frac{\sqrt{3}}{2} & 0 & 0 & 0 & 0 \\ 0 & 0 & 0 & \frac{3}{2} & \frac{3}{2} & 0 & 0 \\ 0 & 0 & 0 & 0 & 0 & \frac{3}{2} & \frac{3}{2} \end{pmatrix} \tag{27}$$

The cost function can be written as

$$J(l+1) = \left\| \begin{bmatrix} i_d^*(l+1) \\ i_q^*(l+1) \\ i_b^*(l+1) \\ i_{sc}^*(l+1) \end{bmatrix} - \begin{bmatrix} i_d(l+1) \\ i_q(l+1) \\ i_b(l+1) \\ i_{sc}(l+1) \end{bmatrix} \right\|_2^2 + \lambda \left\| \Delta v(l) \right\|_2^2 + f \tag{28}$$

Substituting (21)-(27) into (28), the cost function can be rewritten as follows:

$$J = \left\| \Gamma x(k) + \Upsilon U(k) - \Omega(k) \right\|_2^2 + \lambda \left\| SU(k) - Ev(k-1) \right\|_2^2 \tag{29}$$

where

$$\Omega(k) = Y^*(k) - \Pi \tag{30}$$

$$S = \begin{bmatrix} I & 0 & \dots & 0 \\ -I & I & \dots & 0 \\ 0 & -I & \dots & 0 \\ \vdots & \vdots & \vdots & \vdots \\ 0 & 0 & \dots & I \end{bmatrix}, \ E = \begin{bmatrix} I \\ 0 \\ 0 \\ \vdots \\ 0 \end{bmatrix} \tag{31}$$

The cost function can be rewritten as

$$J = \xi(k) + 2(\Xi(k))^{\mathrm{T}} U(k) + U(k)^{\mathrm{T}} Q U(k) \tag{32}$$

where

$$\xi(k) = \left\| \Gamma x_{dq}(k) - \Omega(k) \right\|_2^2 + \lambda \left\| Ev(k-1) \right\|_2^2 \tag{33}$$

$$\Xi(k) = \left((\Gamma x_{dq}(k) - \Omega(k))^{\mathrm{T}} \Upsilon - \lambda (Ev(k-1))^{\mathrm{T}} S \right)^{\mathrm{T}} \tag{34}$$

$$Q = \Upsilon^{\mathrm{T}} \Upsilon + \lambda S^{\mathrm{T}} S \tag{35}$$

After rearrangement, the cost function can be expressed in the form of least squares as follows:

$$J = \left(U(k) + Q^{-1}\Xi(k)\right)^{\mathrm{T}} Q \left(U(k) + Q^{-1}\Xi(k)\right) + c(k) \tag{36}$$

where $c(k)$ is a constant term, which changes only when the sampling time changes. Matrix Q satisfies the properties of symmetry and positive definite, so there is a reversible lower triangular matrix H satisfying

$$H^{\mathrm{T}}H = Q \tag{37}$$

Let $U_{unc}(k) = -HQ^{-1}\Xi(k)$, and the final switch selection can be transformed into a least squares problem:

$$U_{opt}(k) = \arg\min_{U(k)} \|HU(k) - U_{unc}(k)\|_2^2 \tag{38}$$

5. **Simulation.** In order to verify the effectiveness and superiority of the finite set based model predictive controller and power allocation strategy proposed in this paper in the warship DC micro-grid, the control effect of the algorithm is verified by simulation experiments in this section. Firstly, the warship DC micro-grid system is built in Matlab/Simulink environment. The basic parameters of energy supply unit and power converter are shown in Table 1. The equivalent resistance and inductance of the generator can be calculated according to the output voltage, current and power factor. The equivalent resistance and inductance of the battery and super capacitor can be calculated from the measured internal resistance data and the measured charge-discharge data. Some other parameters are selected from the empirical data in the existing research.

Table 1. Warship DC micro-grid system parameters

Parameter	Numerical value	Parameter	Numerical value
Resistance R	5 mΩ	Propeller diameter D	40 cm
Inductance L	30 mH	Seawater density ρ	1018 kg/m^3
Resistance R_1	20 mΩ	Resistance torque coefficient k_t	0.01
Inductance L_1	5 mH	Generator capacity, voltage	1 MW, 380 V
Resistance R_2	20 mΩ	Maximum climbing power $P_{c,g}$	240 kW/min
Inductance L_2	5 mH	Super capacitor capacitance, voltage	500 F, 500 V
Capacitance C	25 mH	Battery capacity, voltage	800 Ah, 500 V

The load power demand curve is shown in Figure 3. According to the power distribution strategy in Section 3, the load on the DC bus is distributed to the generator, battery and super capacitor, in which the system sampling time $T_s = 10$ μs and the time constant of the first-order low-pass filter $\tau = 1$ μs. The distribution results are shown in Figure 4.

Finally, the designed controller is substituted into the control system, and the PWM control power converter action is obtained. Set the rated voltage of DC bus of warship micro-grid $U_{dc}^* = 800$ V, the simulation is carried out around the goal of stabilizing the DC bus voltage and controlling the output reference power of the power converter.

The control effect of the finite control set model predictive controller is shown in Figure 5 and Figure 6. It can be seen that in the stage of $t < 2$ min, the service load gradually increases to about 100 kW; in the stage of $2 \leq t < 5$ min, the propeller starts and accelerates gradually, and the load on the bus increases gradually, but it does not exceed the regulation capacity of the generator, and the hybrid energy storage system does not need to participate in the regulation of output; during the period of $5 \leq t < 10$ min, the sudden change of propeller speed makes the load on the bus fluctuate greatly. Due to

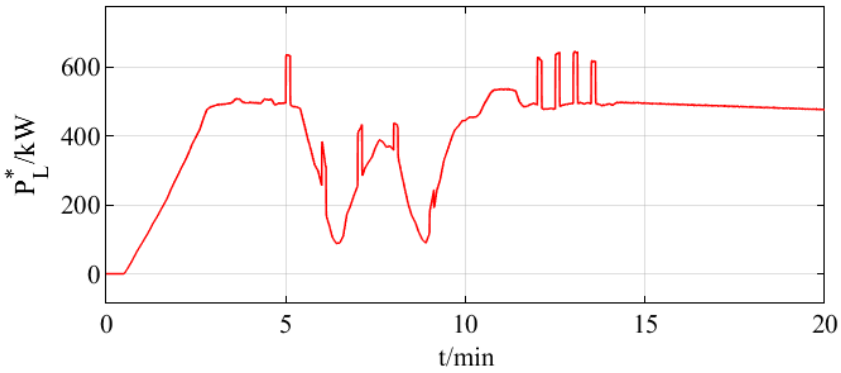

FIGURE 3. Load power demand curve

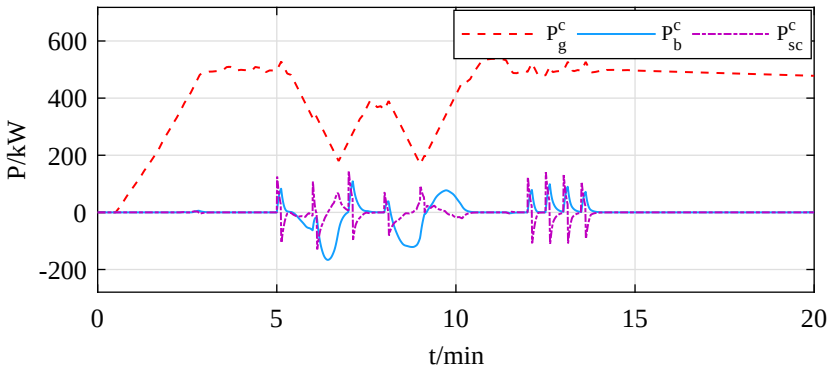

FIGURE 4. Reference power curve of each unit

the limitation of generator climbing power, the output will be insufficient, and a hybrid energy storage system is required to make up for the differential power; at the stage of $10 \leq t < 15$ min, the electromagnetic weapon is put into use, which brings pulse load to the bus. At this time, the super capacitor is charged and discharged rapidly, and the battery cooperates to meet the load demand. In the whole simulation stage, the DC micro-grid system can respond quickly to the load, and the power fluctuation is only within 0.3 kW when reaching the steady state.

Figure 5 shows the output power tracking of the battery. It can be seen that the battery can track the reference power quickly and accurately in the whole process. When $t < 5$ min, the battery does not need to output power, and the steady-state tracking error is only 0.2 kW. Then it participates in the system load regulation, in which the power

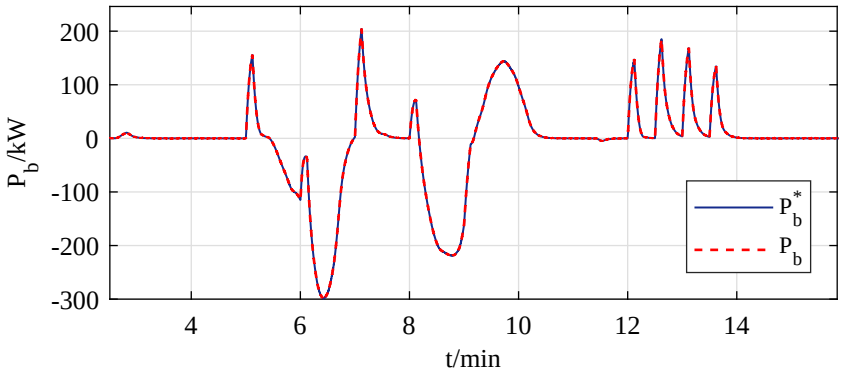

FIGURE 5. Battery output power tracking curve

command P_b^c changes slowly, but the adjustment time of the battery is longer than that of the super capacitor, and the actual output power is around 0.3 kW above and below the reference power.

Figure 6 shows the output power tracking curve of the super capacitor. The super capacitor bears the high-frequency part of the differential power and P_{sc}^c changes more suddenly than the battery, especially in the stage when the electromagnetic weapon is put into use, but the super capacitor can also perfectly track the command, output sufficient power, and keep the steady-state error within 0.2 kW.

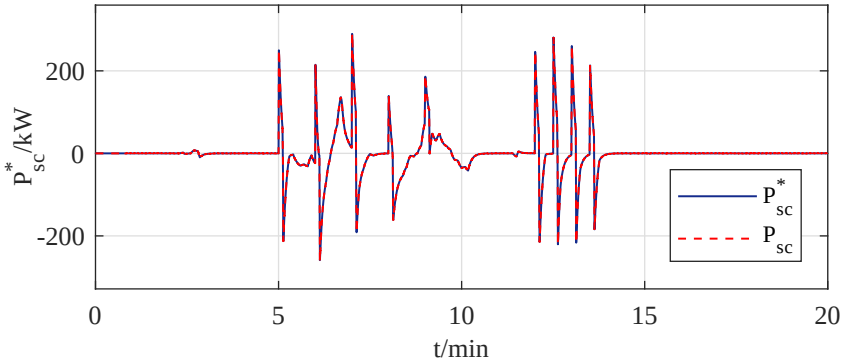

FIGURE 6. SC output power tracking curve

Figure 7 shows the DC bus voltage. As the figure shown, when a pulse load is added to the load, the DC bus voltage can be stabilized between 796 V and 801 V. The reference value of DC bus voltage is 800 V, and its fluctuation can be maintained within 5 V. From here we can see that FCS-MPC has a good control effect on the DC bus voltage of warship micro-grid.

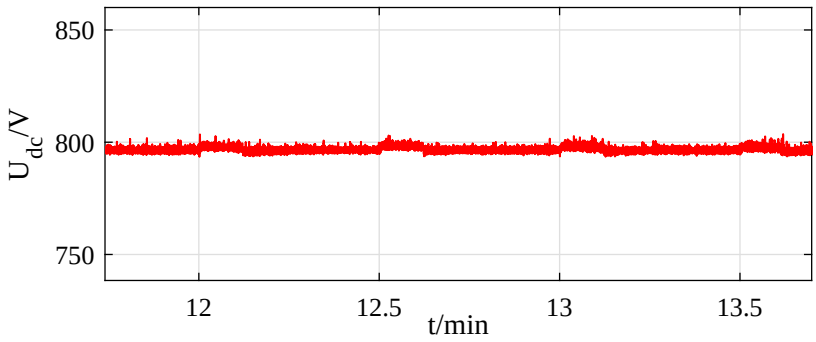

FIGURE 7. DC bus voltage

In [18], Zhang and Yang made a detailed comparison of FCS-MPC based on traversal method, sector division method and least square method. Ergodic method usually needs to traverse all switch combinations when determining the switch state at the next time, so the amount of calculation is large, which affects the effect of real-time control. Therefore, a sector division method can be applied to reducing the number of switch combinations that the algorithm needs to traverse on the selection switch by finding the sector where the desired voltage vector is located. The sector partition method reduces the amount of calculation of finite control set model predictive control. However, under the same experimental conditions, the control effect is worse than the traditional ergodic method. Using a control strategy based on least square method can facilitate the selection of the

best switching state. The simulation results show that under the same test conditions, the control effect of the least square method is better than that of the sector method.

6. **Conclusions.** Due to the sudden change of load, it is difficult for the generator to respond quickly to the restriction of collecting and climbing power, which will easily lead to power imbalance between the power generation side and power consumption side of the warship, resulting in the fluctuation of DC bus voltage. In order to solve this problem, a hybrid energy storage device is introduced into the warship DC micro-grid to make up for the insufficient output of the generator. In this paper, a model predictive control strategy based on finite control set is designed. Firstly, the mathematical model of warship DC micro-grid is established, then the load power is reasonably distributed, and finally the controller is applied to the power converter. It can be seen from the simulation results that the DC bus voltage can be stable near the rated value and is less affected by load fluctuation, whether sudden load addition, load rejection or the use of electromagnetic weapons.

The later work will focus on the research of more efficient power distribution control strategy, and improve the model predictive controller based on finite control set to obtain better control results.

Acknowledgment. This work is supported by the project of Natural Science Foundation of Beijing, China (Grant No. 21JC0026). The authors also gratefully acknowledge the helpful comments and suggestions of the reviewers, which have improved the presentation.

REFERENCES

[1] D. Xu, W. Zhang, W. Yang and Y. Xia, Sliding mode backstepping control of warship DC micro-grid terminal based on preset performance, *Control Theory and Application*, vol.38, no.6, pp.697-706, 2021.

[2] Y. Peng and K. Lu, PMSM speed loop PI self-tuning control based on model prediction, *Motor and Control Applications*, vol.48, no.6, pp.37-43, 2021.

[3] Y. Luo, S. Wang, D. Yang, B. Zhou and T. Liu, Direct prediction compensation strategy of unified power quality conditioner based on FCS-MPC, *IET Generation*, vol.14, no.22, pp.5020-5028, 2020.

[4] J. Liu, S. Cheng, Y. Liu and A. Shen, FCS-MPC for a single-phase two-stage grid-connected PV inverter, *IET Power Electronics*, vol.12, no.4, pp.915-922, 2019.

[5] S. S. Lee and Y. E. Heng, Current controller of three-phase VSI using FCS-MPC with optimal active and zero vector selection for balanced loss distribution and switching loss reduction, *International Transactions on Electrical Energy Systems*, vol.27, no.2, e2250, 2017.

[6] R. K. Sang, K. D. Jin, K. H. Sang, B. C. Jin, K. J. Rae, J. Y. Gyu and K. H. Chan, MPC based energy management system for hosting capacity of PVs and customer load with EV in stand-alone microgrids, *Energies*, vol.14, no.13, 4041, 2021.

[7] A. S. Samosir and A. H. M. Yatim, Implementation of dynamic evolution control of bidirectional DC-DC converter for interfacing ultracapacitor energy storage to fuel-cell system, *IEEE Transactions on Industrial Electronics*, vol.57, no.10, pp.3468-3473, 2010.

[8] B. Wang, V. R. K. Kanamarlapudi, L. Xian, X. Peng, K. T. Tan and P. L. So, Model predictive voltage control for single-inductor multiple-output DC-DC converter with reduced cross regulation, *IEEE Transactions on Industrial Electronics*, vol.63, no.7, pp.4187-4197, 2016.

[9] D. C. Lee, G. M. Lee and K. D. Lee, DC-bus voltage control of three-phase AC/DC PWM converters using feedback linearization, *IEEE Transactions on Industry Applications*, vol.36, no.3, pp.826-833, 2000.

[10] A. Marcos-Pastor, E. Vidal-Idiarte, A. Cid-Pastor and L. Martlnez-Salamero, Loss-free resistor-based power factor correction using a semi-bridgeless boost rectifier in sliding-mode control, *IEEE Transactions on Power Electronics*, vol.30, no.10, pp.5842-5853, 2015.

[11] J. Liang, H. Wang and Z. Yan, Grid voltage sensorless model-based predictive power control of PWM rectifiers based on sliding mode virtual flux observer, *IEEE Access*, no.7, pp.24007-24016, 2019.

[12] J. Huang, A. Zhang, H. Zhang, Z. Ren, J. Wang, L. Zhang and C. Zhang, Improved direct power control for rectifier based on fuzzy sliding mode, *IEEE Transactions on Control Systems Technology*, vol.22, no.3, pp.1174-1180, 2014.
[13] J. Li, M. Wang, J. Wang, Y. Zhang, D. Yang, J. Wang and Y. Zhao, Passivity-based control with active disturbance rejection control of vienna rectifier under unbalanced grid conditions, *IEEE Access*, no.8, pp.76082-76092, 2020.
[14] J. Rodriguez, J. Pontt and C. Silva, Predictive control of three-phase inverter, *Electronics Letters*, vol.40, no.9, pp.561-563, 2004.
[15] H. A. Young, M. A. Perez, J. Rodriguez and H. Abu-Rub, Assessing finite-control-set model predictive control: A comparison with a linear current controller in two-level voltage source inverters, *IEEE Industrial Electronics Magazine*, vol.8, no.1, pp.44-52, 2014.
[16] C. Yu and S. Liang, Model predictive control for a 3DOF laboratory helicopter based on disturbance prediction, *ICIC Express Letters, Part B: Applications*, vol.8, no.2, pp.429-436, https://doi.org/10.24507/icicelb.08.02.429, 2017.
[17] P. Karamanakos, T. Geyer, T. Mouton and R. Kennel, Computationally efficient sphere decoding for long-horizon direct model predictive control, *2016 IEEE Energy Conversion Congress and Exposition (ECCE)*, 2016.
[18] W. Zhang and W. Yang, Model predictive control method of permanent magnet synchronous motor based on finite control set, *Automation Instrument*, vol.41, no.5, pp.42-49, 2020.

Author Biography

Zeliang Hao received his B.Sc. degree in automation from Jiangnan University, China, in 2019. He is currently pursuing his M.Sc. degree in control science and engineering in Jiangnan University. His main research interest is new energy power generation technology.

Youqin Chen received her B.Sc. degree in automation from Jiangnan University, China, in 2019. She is currently pursuing her M.Sc. degree in electrical engineering in Jiangnan University. Her main research interest is new energy power generation technology.

Tinglong Pan received his B.Eng. degree in industrial automation from China University of Mining and Technology, Xuzhou, China, in 1999, and the Ph.D. degree in power electronics and power drive from China University of Mining and Technology, Xuzhou, China, in 2004. He is currently a Professor at Jiangnan University, and his research interests include microgrid control technology, power conversion technology, power drive system and its intelligent control technology.

Weilin Yang received his B.Eng. degree in machine design & manufacture and their automation from University of Science and Technology of China, Hefei, China, in 2009, and the Ph.D. degree in mechanical engineering from City University of Hong Kong, Hong Kong SAR in 2013. He was a postdoctoral researcher at Masdar Institute of Science and Technology (now Khalifa University), Abu Dhabi, UAE, 2013-2016. He was a research engineer of General Electric (GE) Global Research, Shanghai, 2016-2017. He joined Jiangnan University in July 2017, where he is currently an Associate Professor. His research interests include modeling and control of energy systems, robust model predictive control, and dada-driven control.

Xichao Zhou senior engineer, senior researcher of the Science and Technology R&D Center of State Grid Integrated Energy Service Group Co., Ltd., mainly engaged in energy storage system integration technology research.